

TABLE IV. Landau parameters.

r_s	Present approximation			Random-phase approximation		
	F_0^s	F_0^a	F_1^s	F_0^s	F_0^a	F_1^s
1	-0.271	-0.248	-0.360	-0.199	-0.165	-0.096
2	-0.481	-0.417	-0.606	-0.363	-0.243	-0.024
3	-0.656	-0.543	-0.792	-0.541	-0.307	0.078
4	-0.805	-0.634	-0.924	-0.740	-0.359	0.192
5	-0.937	-0.693	-0.993	-0.963	-0.406	0.315
6	-1.063	-0.722	-0.984	-1.212	-0.451	0.444

$$F_i^{s(a)} = \frac{m^* p_F \Omega}{\pi^2} \frac{2l+1}{2} \int_{-1}^1 f^{s(a)}(\cos\theta) P_l(\cos\theta) d\cos\theta, \quad (7.2)$$

where P_l is a Legendre polynomial. It can be shown that

*Issued as N.R.C.C. Report No. 12182.

†National Research Council Postdoctorate Fellow 1969-71. Present address: Max-Planck-Institut für Physik und Astrophysik, 8 München 23, Föhringer Ring 6, Germany.

¹M. Gell-Mann, Phys. Rev. **106**, 369 (1957).

²K. A. Brueckner and K. Sawada, Phys. Rev. **112**, 328 (1958).

³S. D. Silverstein, Phys. Rev. **128**, 631 (1962); **130**, 1703 (1963).

⁴T. M. Rice, Ann. Phys. (N. Y.) **31**, 100 (1965).

$$c_V/c_V^0 = 1 + \frac{1}{3}F_1^s,$$

$$\chi/\chi^0 = (1 + \frac{1}{3}F_1^s)/(1 + F_0^a), \quad (7.3)$$

$$\kappa_T^0/\kappa_T = (1 + F_0^s)/(1 + \frac{1}{3}F_1^s).$$

From the results of Secs. IV-VI we obtain a set of Landau parameters as shown in Table IV. The effective mass is, of course, given by the specific heat. Another parameter, the quasiparticle renormalization constant Z , has previously been calculated in connection with the momentum distribution.¹¹

ACKNOWLEDGMENTS

The author is grateful to Dr. C. Mavroyannis for reading the manuscript, and to the National Research Council of Canada for its support and hospitality.

⁵L. Hedin, Phys. Rev. **139**, A796 (1965).

⁶J. Lam, Phys. Rev. B **3**, 1910 (1971).

⁷L. D. Landau, Zh. Eksperim. i Teor. Fiz. **30**, 1058 (1956) [Sov. Phys. JETP **3**, 920 (1957)].

⁸In Ref. 6, at the end of Sec. V, it is incorrectly stated that $f(0)$ is finite.

⁹R. Dupree and D. J. W. Geldart, Solid State Commun. **9**, 145 (1971).

¹⁰K. S. Singwi, M. P. Tosi, R. H. Land, and A. Sjölander, Phys. Rev. **176**, 589 (1968).

¹¹J. Lam, Phys. Rev. B **3**, 3243 (1971).

Phonon Spectra of Some Transition Metal Carbides from a Simple Pseudopotential Approach*

M. Mostoller

Solid State Division, Oak Ridge National Laboratory, Oak Ridge, Tennessee 37830

(Received 23 September 1971)

It is shown that many of the over-all features of the phonon spectra of transition metal carbides and related compounds can be approximately reproduced by a simple dielectric-response approach which uses Heine-Abarenkov pseudopotentials and free-electron screening, although the model calculations do not show the unusual structure seen in some of these materials. Illustrative applications are made to UC, HfC, TaC, and NbC.

I. INTRODUCTION

Smith and Gläser's^{1,2} recent measurements of the phonon spectra of several transition metal carbides have deepened the already widespread interest in these and related compounds. Generally, the transition metal carbides are very hard, have high melting points, and display metallic conductivity. Furthermore, some are superconductors with transition temperatures higher than the pure metals, and the occurrence of superconductivity is

apparently correlated with the number of outer-shell electrons present. Although similar in some respects, the phonon spectra of these materials exhibit considerable variety: The splitting between optical and acoustical modes is substantially greater in some compounds (TaC) than in others (HfC), dispersion in the optical branches may be relatively small (UC) or large (HfC), and unusual structure is seen in the phonon spectra of the superconductors (TaC, NbC) above and below the transition temperature.

A variety of approaches may be employed to attempt to fit the observed dispersion curves. Because of their metallic behavior, it was felt desirable to look at the phonon spectra of the transition metal carbides and related compounds from the perspective of a screened-pseudopotential or dielectric-response approach. This paper presents illustrative results of simple first attempts at such calculations. These results are comparable to those obtained by Weber and Bilz,³ who used a shell model modified to eliminate the Lyddane-Sachs-Teller splitting of the optical modes at $q = 0$ by treating the conduction electrons as a perturbation.

II. MODEL FOR CALCULATIONS

The dielectric-response approach has been applied with some success to the phonon spectra of a variety of materials, including, for example, the alkali metals,⁴ magnesium⁵ and aluminum,⁶ and the group-IV semiconductors.^{7,8} The materials of interest here present special difficulties, in that the outer unfilled shells contain d or f electrons, and directional metal-nonmetal bonds are thought to play an important role in their properties.^{2,3,9,10} Although such features can be included in screened-pseudopotential calculations, at least phenomenologically, it is instructive to see how well a very simple approach works before attempting a more ambitious treatment. Accordingly, we use simplified Heine-Abarenkov pseudopotentials,^{11,12} with free-electron random-phase-approximation (RPA) screening incorporating a parametrized correlation correction.⁵

For an electron interacting with the ion at site b in the (zeroth) unit cell, the pseudopotential is taken to be

$$v_b(r) = -A_b, \quad r < r_b,$$

$$= -Z_b e^2 / r, \quad r > r_b. \quad (1)$$

The corresponding pseudopotential transform or form factor is

$$v_b(p) = -\frac{4\pi Z_b e^2}{p^2} \left[\left(1 - \frac{r_b}{R_b}\right) \cos pr_b + \frac{r_b}{R_b} \frac{\sin pr_b}{pr_b} \right], \quad (2)$$

with R_b defined by $A_b = Z_b e^2 / R_b$. Expressed in terms of the ratio $x = k/k_F$ of the electron momentum to the Fermi momentum, the electron screening function is given by

$$\epsilon(k) = 1 + \frac{\gamma_{FT}^2}{x^2} \alpha(x) \left(1 - \frac{x^2}{2(\eta + x^2)}\right), \quad (3)$$

$$\alpha(x) = \frac{1}{2} \left(1 - \frac{x^2 - 4}{4x} \ln \left| \frac{x+2}{x-2} \right| \right), \quad (4)$$

where γ_{FT} is the ratio of the Fermi-Thomas and the Fermi momenta,

$$\gamma_{FT}^2 = k_{FT}^2 / k_F^2 = 4me^2 / \pi \hbar^2 k_F. \quad (5)$$

The ionic charges, well radii, and well depths Z_b , r_b , and A_b , and the electronic correlation-correction factor η ¹³ are treated as adjustable parameters, and k_F is determined by

$$k_F = (3\pi^2 \sum_b Z_b / \Omega_0)^{1/3}, \quad (6)$$

where Ω_0 is the unit cell volume.

A least-squares fitting procedure allowing sequential and/or simultaneous variation of the adjustable parameters was used to fit the experimental data at selected points in the Brillouin zone. The fitting procedure was highly nonlinear, and the seven variable parameters were clearly not a linearly independent set. Variation of the correlation-correction factor η was found to produce relatively small changes in the dispersion curves, so its value was fixed by $\eta = 1 + \gamma_{FT}^2$ in all but the last few runs for a particular crystal, if it

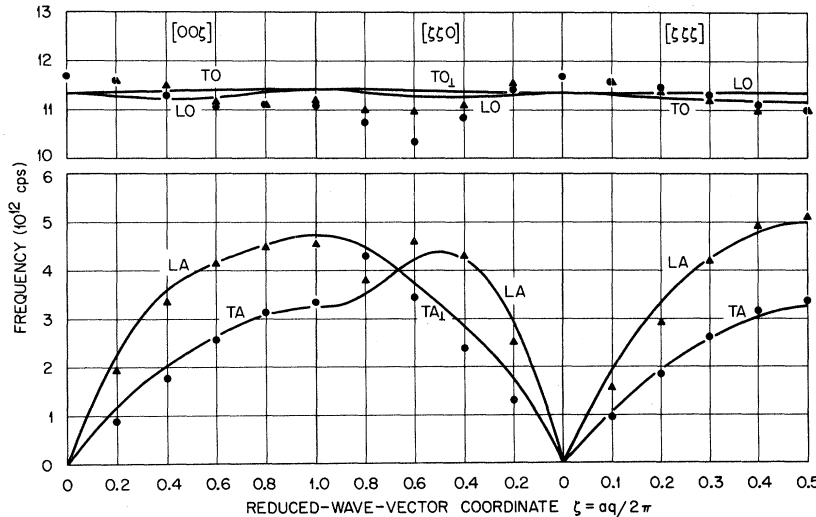


FIG. 1. Phonon spectra of UC.

was varied at all.

III. RESULTS

Figures 1-4 show the results obtained for UC, HfC, TaC, and NbC, respectively. The model parameters for the materials, all of which have the NaCl structure, are listed in Table I.

For UC, the agreement between calculated and experimental values is reasonably good, generally to within a few percent. One apparent qualitative discrepancy is that the calculated optical modes fall in the wrong order along all three symmetry directions, particularly along the $(\xi\xi0)$ direction, where the experimental ordering is unequivocal. This inversion of the optical modes also occurs in the fit to the UC spectra obtained with a second-neighbor Born-von Karman model,² which is perhaps slightly better than that shown in Fig. 1.

The calculated results for HfC shown in Fig. 2 are in excellent agreement with the measured values at $q=0$ and the $(00\xi)-(\xi\xi0)$ zone boundary, but the calculated longitudinal modes do not exhibit as much dispersion as is observed. The fit to the acoustical branches is not quite as good as that of Weber and Bilz,³ but the fit to the optical modes is much better. It should be noted, however, that they did a single representative calculation for both

HfC and TaC despite the differences in shape and scaling of the optical modes in the two crystals, perhaps because there was not as much experimental information available for HfC at the time.

As shown in Fig. 3, the simple screened-pseudopotential model gives fairly good agreement with some over-all features of the TaC dispersion curves, but it is not surprising that it cannot even approximately replicate the unusual structure seen in these spectra. The pseudopotential results are superior to those obtained by second-neighbor Born-von Karman analysis, and are comparable to the modified-shell-model results of Weber and Bilz. As can be seen in Table I, the electronic parameter η was not varied from the value $1 + \gamma_{FT}^2$ in the UC and HfC calculations, but variation of η (in a direction which reduces the magnitude of the correction to the screening) was found to be helpful for TaC. However, since the dependence on η is relatively weak, rather large changes in η may occur in fitting selected frequencies, and the large value $\eta = 10.56 \approx 5(1 + \gamma_{FT}^2)$ for TaC illustrates this point. If the other parameters for TaC are held fixed at the values given in Table I, but $\eta = 1 + \gamma_{FT}^2 = 2.183$ is used rather than $\eta = 10.56$, the calculated frequencies change by the order of 10% or less. The major qualitative difference observed is that

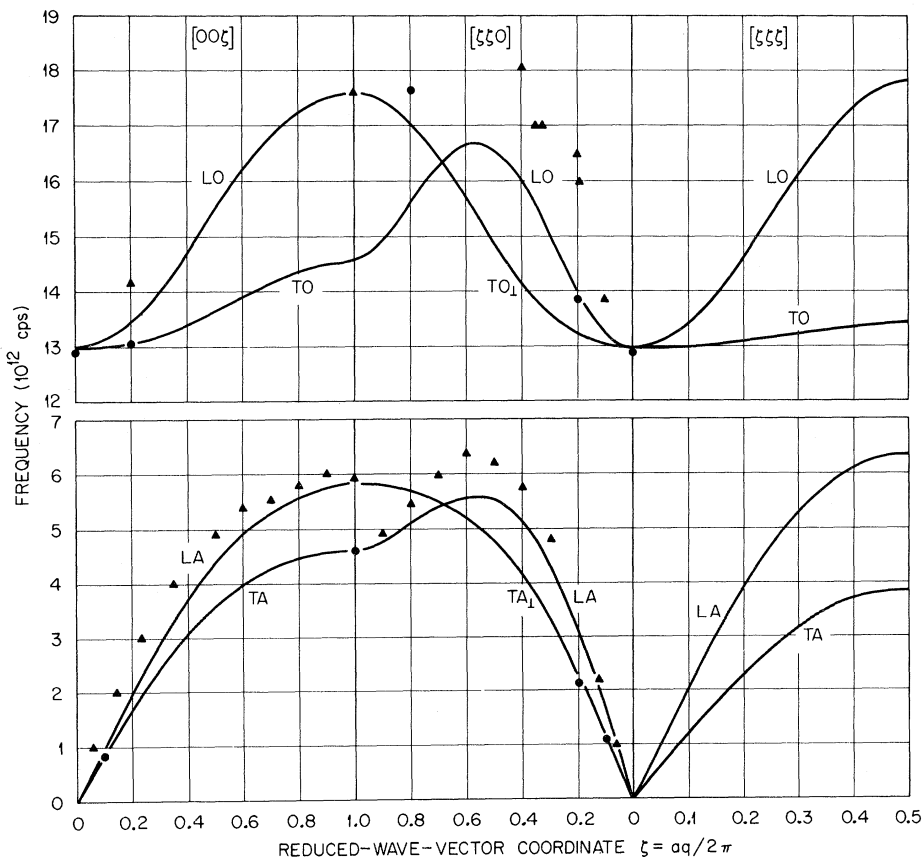


FIG. 2. Phonon spectra of HfC.

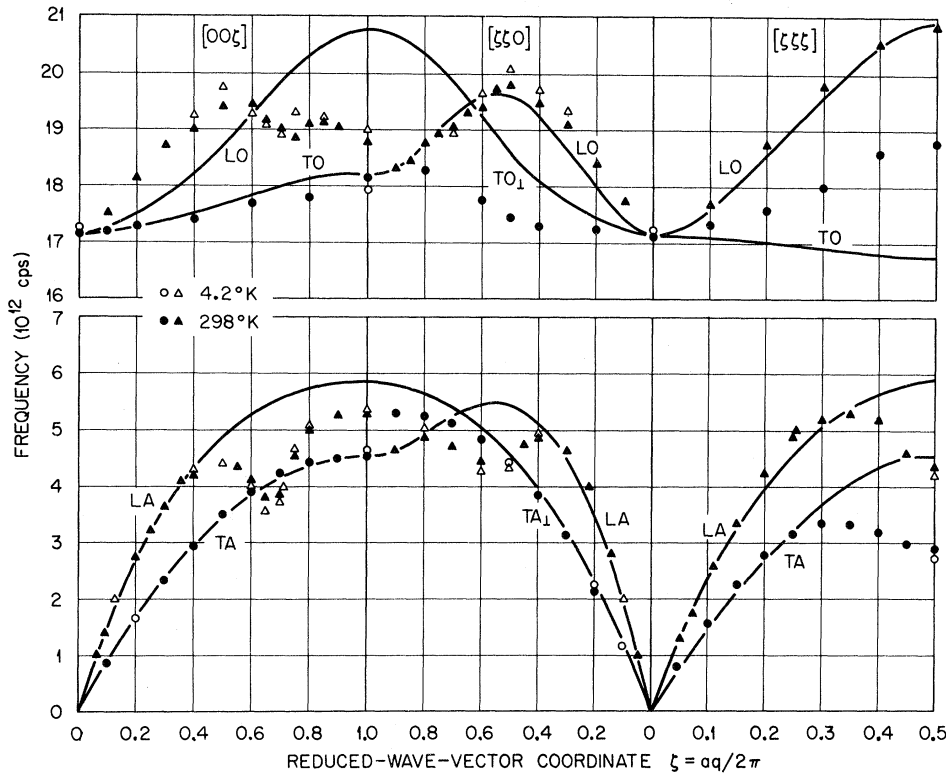


FIG. 3. Phonon spectra of TaC.

the optical modes shift upward at $q = 0$ and lose most of their dispersion: $\nu(0)$, $\nu_{LO}(0, 0, 1)$ and $\nu_{LO}(\frac{1}{2}, \frac{1}{2}, \frac{1}{2})$ have values of 18.62, 18.87, and 18.90 $\times 10^{12}$ cps respectively for $\eta = 2.183$, compared with the values 17.15, 20.77, and 20.95 $\times 10^{12}$ cps for $\eta = 10.56$.

Rather than attempting to fit their measured dispersion curves, the calculations for NbC and NbC_{0.76} were done by scaling the TaC parameters. Along with the change in the mass of the metal ion, the ionic radii r_b and R_b for NbC were scaled from their values for TaC by the ratio $a(\text{NbC})/a(\text{TaC})$ of the lattice constants, so that the form factors [cf. Eq. (2)] would be unchanged as a function of $\xi = q/(2\pi/a)$. For NbC_{0.76}, the well radii r_b and the niobium well-depth parameter R_{Nb} were found from the NbC values by multiplying by $a(\text{NbC}_{0.76})/a(\text{NbC})$, and a very rough attempt was made to account for the deviation from stoichiometry by reducing the carbon mass, charge, and well depth A_c from their values in NbC by the factor 0.76. For both NbC and NbC_{0.76}, $\eta - 1$ was taken to scale from TaC as $\gamma_{\text{FT}}^2 \propto a/(\sum Z_b)^{1/3}$. Results for the acoustic modes are shown in Fig. 4, in which the scaled NbC curves are compared with the data for NbC_{0.98}. The optical modes are not shown because the curves are quite similar to those for TaC, but with somewhat less dispersion; at $q = 0$, the calculated frequencies for NbC and NbC_{0.76} are 17.54 and 17.90 $\times 10^{12}$ cps, respectively, while the ex-

perimental values are 16.65 and about 17.65 $\times 10^{12}$ cps. From Fig. 4, it would appear that simple scaling laws are reasonably well obeyed in the transition metal carbides.

In view of the crudeness of the calculational model, caution should be exercised in attempting to extract physical content from the parameters listed in Table I. For example, the effective metal ion charges in Table I are quite a bit larger than the effective carbon charges, and a substantial fraction of the outer-shell electrons apparently does not participate in the screening. This may be taken to indicate localization of much of the electronic charge density, with a net transfer of charge toward the carbon sites. However, curves similar to those in Figs. 1-4 can also be generated by (roughly) exchanging the metal ion and carbon pseudopotential parameters, although the quality of the fits deteriorates and effective carbon charges greater than 4 are requested by the least-squares fitting routines in some cases.

IV. CONCLUSIONS

It has been shown that a simple dielectric-response approach can reproduce many of the overall features of the phonon spectra of representative transition metal carbides and related compounds. To obtain a better description of the lattice vibrations in these materials, a number of directions may be taken. One very simple possi-

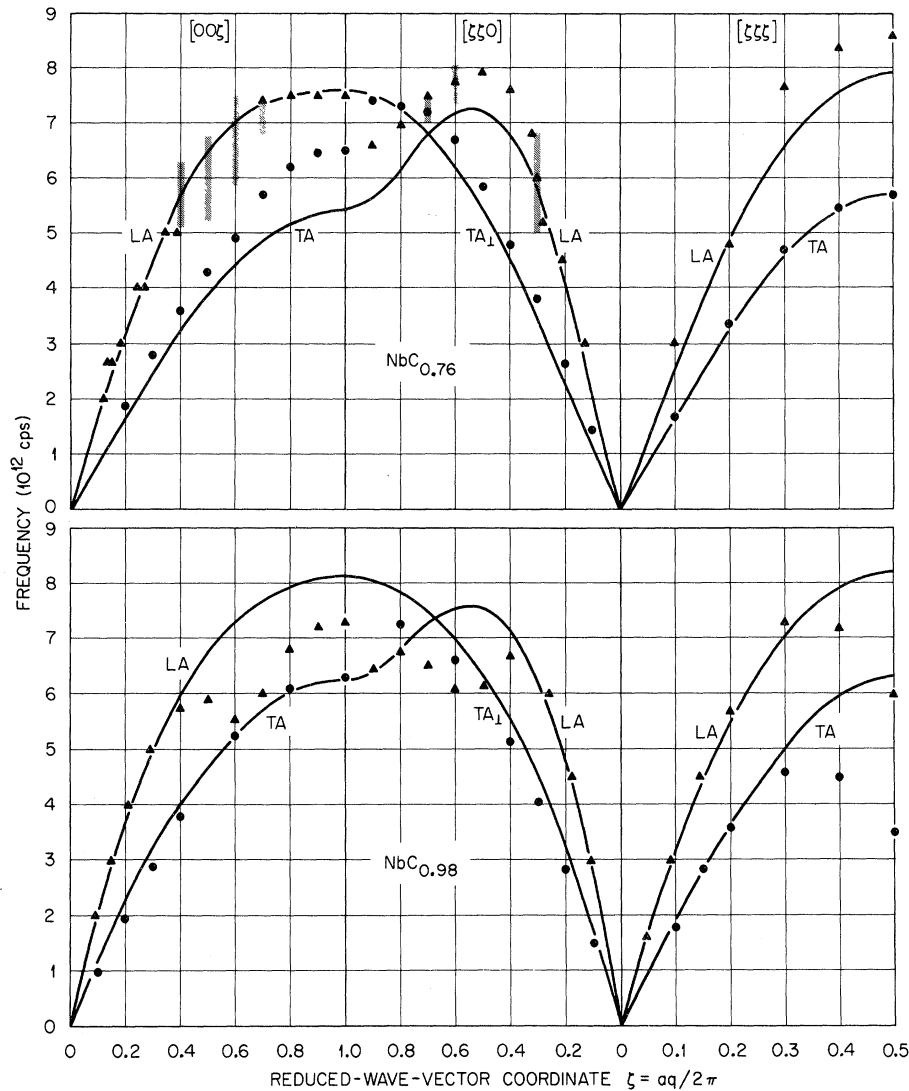


FIG. 4. Acoustic phonon spectra of $\text{NbC}_{0.98}$ and $\text{NbC}_{0.76}$. The calculated curves are for NbC and $\text{NbC}_{0.76}$, scaled from TaC as explained in the text.

TABLE I. Pseudopotential-model parameters for crystals MC . The lattice constants a and the well width and depth radii r_b , R_b are in \AA and the well depths A_b are in eV.

	UC	HfC	TaC	NbC	$\text{NbO}_{0.76}$ ^a
a	4.96	4.64	4.4555	4.47	4.44
Z_M	5.087	3.694	3.598	3.598	3.598
A_M	18.13	26.16	35.06	34.95	35.18
r_M	0.900	0.950	0.856	0.859	0.854
R_M	4.040	2.034	1.478	1.482	1.473
Z_C	1.336	1.705	2.683	2.683	2.039
A_C	32.51	55.88	64.07	63.86	64.29
r_C	1.078	1.093	1.166	1.170	1.162
R_C	0.592	0.439	0.603	0.605	0.605
η	2.307	2.296	10.560	10.591	11.439
$1 + \gamma_{FT}^2$	2.307	2.296	2.183	2.187	2.222

^aFor $\text{NbC}_{0.76}$, a negative ion mass of $9.12 \text{ amu} = 0.76M_C$ was used.

bility is to add short-range interactions to the screened-pseudopotential model to include core-core interactions and noncentral forces between near neighbors. It can be anticipated, however, that such an approach will not produce structure like that seen in TaC and NbC , and this has been borne out in exploratory calculations by the author. A more general phenomenological dielectric-response treatment^{7,8} might prove fruitful. At a more fundamental level, efforts should be made to include at least the qualitative features of the band structures of these materials¹⁰ in calculations of the electron-screening function. Given the obviously strong interrelationship between their electronic and ionic properties, extensive further experimental and theoretical studies will probably be required before a full understanding of these compounds is achieved.

ACKNOWLEDGMENTS

The author would like to thank H. G. Smith for

initially stimulating and continually encouraging his interest in the problem, and R. F. Wood and H. L. Davis for helpful discussions.

*Research sponsored by the U. S. Atomic Energy Commission under contract with Union Carbide Corporation.

¹H. G. Smith and W. Gläser, *Phys. Rev. Letters* **25**, 1611 (1971).

²H. C. Smith and W. Gläser, in *Proceedings of the International Conference on Phonons, Remes, France, July 1971*, edited by M. Nusimovici (Flammarion Sciences, Paris, 1971).

³W. Weber and H. Bilz, in Ref. 2.

⁴P. S. Ho, *Phys. Rev.* **169**, 523 (1968).

⁵W. F. King and P. H. Cutler, *Phys. Rev. B* **3**, 2485 (1971).

⁶S. H. Vosko, R. Taylor, and G. H. Keech, *Can. J. Phys.* **43**, 1187 (1965).

⁷R. M. Martin, *Phys. Rev. Letters* **21**, 536 (1968).

⁸S. K. Sinha, R. P. Gupta, and D. L. Price, *Phys. Rev. Letters* **26**, 1324 (1971).

⁹R. E. Rundle, *Acta Cryst.* **1**, 180 (1948).

¹⁰H. L. Davis, *Bull. Am. Phys. Soc.* **16**, 637 (1971); Harold L. Davis, in *Plutonium 1970 and Other Actinides*, edited by W. N. Miner (Metallurgical Society, New York, 1970), p. 209.

¹¹V. Heine and I. Abarenkov, *Phil. Mag.* **9**, 451 (1964); I. Abarenkov and V. Heine, *ibid.* **12**, 529 (1965).

¹²W. A. Harrison, *Pseudopotentials in the Theory of Metals* (Benjamin, New York, 1966).

¹³As noted in Ref. 5, values suggested for η in the literature include $\eta=1, 2, 1+\gamma_{FT}^2$.

Theory of Phonon-Aided Optical Absorption in the Alkali Metals. I. Sodium[†]

N. M. Miskovsky

Department of Physics, Altoona Campus, The Pennsylvania State University, Altoona, Pennsylvania 16601

and

P. H. Cutler

Surface Physics Division, European Space Research Organization, Noordwijk, Holland
(Received 12 January 1971)

Using the formalism of Nettel, the optical absorption $\sigma(\omega)$ due to all single-phonon exchange processes has been calculated for sodium from the near-infrared to the near-ultraviolet region, i. e., $\hbar\omega=0.5-4.0$ eV, and at various temperatures. An initial study was made to determine the correct form of wave function to be used in calculating the absorbing power. The Butcher nearly-free-electron theory was reformulated in terms of orthogonalized plane waves (OPW). This investigation led to the conclusions that (i) a single OPW is not adequate to use as a wave function in the calculation of the absorbing power, (ii) the core-induced absorption does not contribute significantly to the interband absorption, and (iii) a nearly-free-electron wave function is adequate to use as a first approximation to calculate $\sigma(\omega)$ for the alkali metals. Consequently, a nearly-free-electron wave function was used in the subsequent calculations of the optical absorption due to single-phonon exchange processes. The phonon spectrum for sodium was calculated throughout the Brillouin zone using the pseudopotential method of Schneider and Stoll. In the infrared and intermediate regions, the results of this first-principles calculation are in excellent agreement with the recent experimental data of Smith, but do not agree with the experimental results of Mayer and Hietel; i. e., (i) there is no evidence in the computed curves for the existence of the anomalous resonance absorption, nor (ii) does this theory obtain the temperature behavior of the anomaly exhibited in the data of Mayer and Hietel. In the interband region the results are also in good qualitative agreement with the data of Smith. The temperature dependence of the computed interband absorption (which enters intrinsically via the phonon occupation operator) is again in disagreement with the data of Mayer and Hietel.

I. INTRODUCTION

The alkali metals have long been regarded as good examples of simple metals whose behavior could be explained using the nearly-free-electron model, i. e., the optical-absorption spectrum should

conform to the traditional Drude theory in the far infrared, an intermediate region dominated by intraband transitions, and a well-defined interband region. However, these metals are highly reactive, and thus it is very difficult to obtain clean surfaces of these materials; therefore, until recently little